PROCEEDINGS, Thirty-Seventh Workshop on Geothermal Reservoir Engineering
Stanford University, Stanford, California, January 30 - February 1, 2012
SGP-TR-194

GEOCHEMISTRY OF A SUB-GLACIAL VOLCANIC HYDROTHERMAL SYSTEM AT MOUNT SPURR, ALASKA

L. Garchar[1], R. Wendlandt[1], B. Martini[2*], L. Owens[2]

[1]Colorado School of Mines, Golden, CO, 80401

[2]Ormat Nevada Inc., 6225 Neil Rd., Reno, NV, 89511

now with Martini Consulting, Richland, WA, 99352

email: laura.garchar@gmail.com

ABSTRACT

Mt. Spurr is an ice and snow-covered andesitic volcano located at the northern extent of the Aleutian arc in south central Alaska. Previous workers (Turner and Wescott, 1986; Martini et al., 2011) have identified a prospective geothermal system on the south side of the volcano, beneath Crater Peak. This research applies mineralogical and aqueous geochemical investigations at Mt. Spurr in order to characterize the hydothermal system, focusing on the possible extent, temperature, origin of fluids, and fluid pathways occurring in the system.

INTRODUCTION

Since at least the 1970s, it has been known that the state of Alaska has a number of proven or speculated geothermal resources (State Long Term Energy Plans 1980-1982, Turner and Wescott, 1986). However, due to the remote location of many potential geothermal fields and lack of energy transmission infrastructure as well as the relatively low price of gas, these resources have remained largely untapped. Now with the increased concern over depletion of natural gas resources in the Cook Inlet and greater awareness to the benefits of renewable energy, ,utilization of geothermal resources in Alaska is more favorable. Alaska's first geothermal power plant, Chena Hot Springs, came online in 2006 and currently produces 680kWe from 165° F fluid (AEA, 2009).

Mt. Spurr's volcanic system has been widely studied by Alaska state agencies. Past and ongoing studies of gas emissions, ice melt, geologic history, seismic activity and geochemistry largely address the hazard of future eruptions. However, Mt. Spurr's active magmatic system, proximity to Anchorage, and the existing power infrastructure in Beluga also make it a prospective geothermal target. The geothermal potential of Mount Spurr has been addressed by Turner and Wescott (1986), and Martini et al (2011). This study examines the geochemistry of spring waters and the mineralogy of core samples taken from exploration drilling at Mt. Spurr over the summer of 2011. Aqueous and mineral geochemistry seems to be related to one another spatially, and allow the distinction between fluids with characteristics of a deep thermal source and those that are dominated by shallow processes like mixing and dilution.

GEOLOGIC SETTING

Mt. Spurr is located about 100km west of Anchorage, in the Tordrillo Mountains on the northwest side of the Cook Inlet (Fig. 1). It is covered by about 67 cubic kilometers of perennial snow and ice, which is about 15 times more snow and ice than is present on Mount Rainier. Several valley glaciers dissect the volcano. Most of the area surrounding this volcano is uninhabited wilderness, and its remote location limits recreational use of the area. (Waythomas and Nye, 2002)

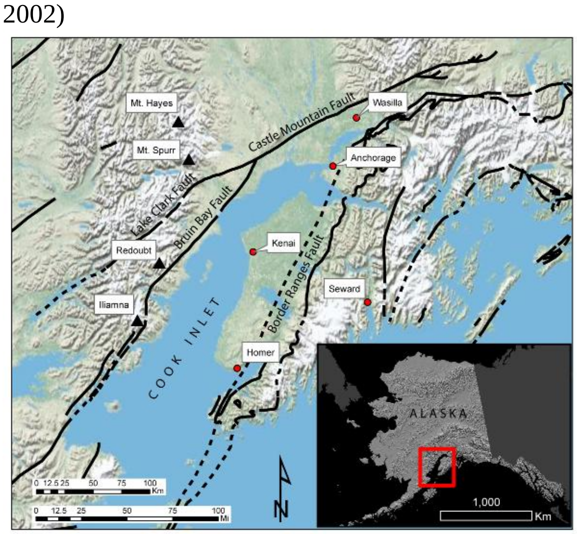

Figure 1. Mt. Spurr is in south-central Alaska on the eastern end of the Aleutian Arc. After Schaefer, 2006.

Nye and Turner (1990) consider the Spurr volcanic complex (SVC) to be representative of eastern Aleutian volcanism, and note that it has a single, mature center that is located on the thickest crust of any Aleutian arc volcano. Additionally, Mt. Spurr is the easternmost active center of the Aleutian arc. The SVC lies on top of continental crust formed by amalgamation of accretionary terranes including Silurian-early Jurassic limestone, basalt and clastic rocks, and Jurassic and/or Cretaceous flysch (Nye and Turner, 1990). All of these rocks have been intruded by the Aleutian range batholith during Jurassic, early Tertiary, and mid-Teriary times (Nye and Turner, 1990). Immediately to the south of Mt. Spurr, the bedrock is granodiorite (62 and 69Ma), while to the north-northeast quartz monzonite intrudes Jurassic-Cretaceous flysch and is faulted against the West Foreland Formation (Nye and Turner, 1990). The West Foreland Formation is a tuffaceous sandstone and conglomerate unit that contains coal beds and underlies the oil and gas producing Kenai Group sediments in the Cook Inlet Basin (Montgomery and Barker, 2003).

The SVC shows evidence of at least four eruptions since the volcano was formed (Nye and Turner, 1990). Ancestral mount Spurr was composed of lava flows and pyroclastic deposits dated around 255,000 to 18,000 years ago. Ancestral Spurr lavas are mostly uniform andesite with 58-60% SiO_2. This ancestral Spurr edifice was destroyed in a Bezymianny-type eruption that produced a horseshoe-shaped caldera, a debris avalanche partially overlain by ash-flow tuff, and two new vents: the current Mt. Spurr, which grew out of the collapsed summit region, and proto-Crater Peak, a breach on the south side of the edifice (Nye and Turner, 1990). The nature of magmatism changed abruptly after the caldera was formed. Two distinct magmas and mixtures of these two have been observed (Nye and Turner, 1990). The current Mount Spurr dome is composed of andesite that is more silicic than that of ancestral Spurr, but contains olivine and amphibole xenocrysts derived from more mafic magma. Lavas from proto-Crater Peak and Crater Peak are consistently more mafic than ancestral Spurr and contain distinctive pyroxenite clots that are not seen in ancestral Spurr samples (Nye and Turner, 1990). Crater Peak has since erupted in recent times, once in 1953 and again in 1992. Both eruptions were Volcanian to sub-Plinian pyroclastic events that generated large volumes of volcanic ash (Waythomas and Nye, 2002). The current Mt. Spurr edifice is shown in Fig. 2.

Regional fault systems may be important to understanding the hydrogeologic framework of Mt. Spurr. The Castle Mountain, Lake Clark, and Bruin Bay faults are all reverse faults with northwest side up and some component of oblique slip. (Finzel et al, 2009). Displacement on the eastern part of the Castle Mountain Fault is up to 1.2km of reverse motion and 130km of right lateral separation since at least the Early Cenozoic, and scarps and historical activity suggest Holocene movement of 2.8-3mm/yr (Finzel et al, 2009). The Lake Clark Fault is estimated to have 500m-1km of vertical offset and 5-26km of right lateral motion since the late Eocene. The Bruin Bay fault has left-lateral motion of 19-65km and vertical motion of at least 3km, but may have less vertical motion near the intersection with the Castle Mountain Fault. Significant motion on the Bruin Bay Fault may be as recent as Quaternary time. (Finzel et al, 2009)

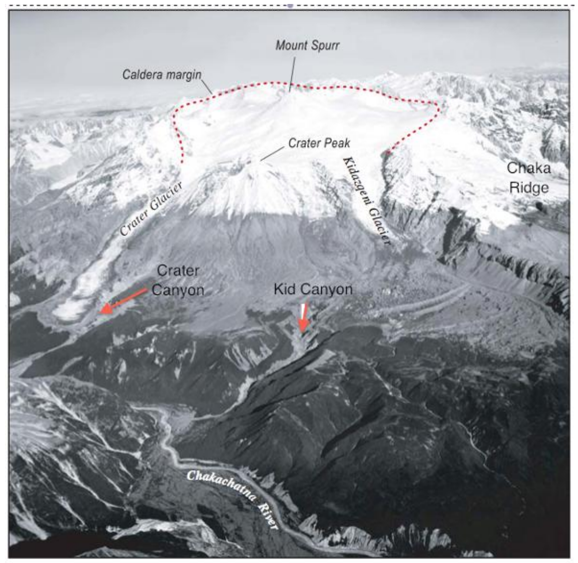

Figure 2. Air photo of Mt. Spurr, showing locations of Crater Peak, Crater Canyon, and Chaka Ridge. Core hole 26-11 is located just out of the field of view to the middle right. Modified from Waythomas and Nye, 2002.

The Capps Glacier Fault juxtaposes Cenozoic granitic rocks to the northwest over gently deformed Cenozoic clastic rocks, apparently of the West Foreland Formation, to the southeast. The Cenozoic clastic rocks unconformably overlie metamorphic basement rocks. Hangingwall granite in fault contact with Cretaceous-Jurassic footwall greenstone along part of the fault implies either dip-slip reverse motion along a high angle structure or oblique-slip motion along a transpressional structure. Displacement could be tens to hundreds of meters. Folded Cenozoic basin deposits to the southeast of the Capps Glacier Fault are oriented obliquely to the fault. Similar oblique orientations of cored anticlines in the Cook Inlet Basin could imply that the Bruin Bay, Castle Mountain, and Capps Glacier faults and associated folds evolved in similar regional stress conditions. (Finzel et al, 2009)

The study area for this research focuses on springs and seeps below Crater Peak and at other locations to the east. Surface elevation mapping, geophysical anomalies, and field studies suggest that several faults cross-cut the study area and likely influence fluid pathways (Martini et al, 2011). One of the goals of this research is to speculate if a possible hydrothermal system below Crater Peak extends further east, where there would be less volcanic hazard involved with possible drilling and development.

METHODS

Water and core samples were collected during a field visit 19 July-4 August 2011 (Fig. 3).

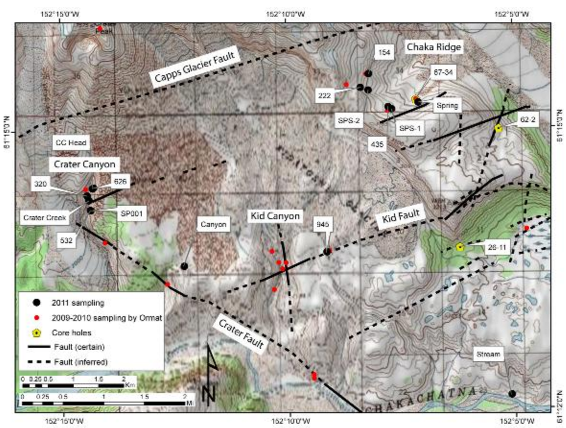

Figure 3. Sampling locations are on the south side of Mt. Spurr, just to the south and east of Crater Peak. Faults, core holes, and previous sampling locations from Martini et al, 2011.

Previous work including sampling from Martini et al (2011) and helicopter-based field accessibility directed the selection of spring sampling locations. At each site, water was extracted by syringe and filtered through a 0.45μm membrane into a suite of bottles for laboratory geochemical analysis of anions, cations, major components, dissolved gas, and stable isotopes. The samples for cation analysis were acidized with 0.02N HNO_3, and samples to be analyzed for H_2S were preserved with 10.15 ZnAc. In addition, field H_2S, SiO_2, alkalinity, temperature, pH, and conductivity were measured. Approximate flow rate was estimated by visual observation.

Anions, cations, and major components were analyzed by the Western Environmental Testing Laboratory; dissolved gas (H_2S) analyses were performed by Thermochem; stable oxygen, hydrogen, carbon (from dissolved inorganic carbon) and sulfur (from sulfate) isotope analyses were conducted at the University of Nevada, Reno; and stable carbon isotope analyses were done at the University of Arizona.

Core hole 26-11 drilled through 50' of colluvium, 587.5' of debris flow, and 3350.5' of sandstones and conglomerates of the West Foreland Formation before reaching a total depth of 3988'. It hit fault zones at 1889-1894', 2022-2024', 2580-2590' and 3216-3224'. Water was encountered at 1690' and 2587' at less than 5gpm. Water flow was brief, however, and it was not possible to recover any samples. The highest measured temperature was 57˚C between 3400-3600'. (Ormat Nevada, Inc., 2011)

Representative samples of conglomerate and sandstone from core hole 26-11 were selected for petrographic analysis at the time of drilling based on the extent of alteration (fresh-altered appearance) and proximity to fault zones. Samples for clay analysis were also selected based on the occurrence of clay material and proximity to fault zones.

Polished thin sections of eight core samples from core hole 26-11 were made and analyzed at the Colorado School of Mines using transmitted optical microscopy. Six of the thin sections are of conglomerate with a sandy matrix, and two are of coarse-grained sandstone intervals of the West Foreland Formation.

Seven clay-rich samples were analyzed by X-ray diffraction at the Colorado School of Mines. The samples were first washed and scrubbed with a toothbrush to minimize possible bentonitic drilling mud contamination. All samples reacted to the water by swelling. Randomly oriented whole rock, oriented clay-sized fraction, and oriented glycolated clay-sized fraction scans were done for each sample. Additionally, some material from core sample "3434" was scraped off and analyzed with oriented scans. This material was from a calcite vein and from the red, mineralized surface of an altered clast. All samples were analyzed from 3-40º 2Θ, and three of the samples were also scanned in the 59-65º 2Θ range.

RESULTS

Water Chemistry

Analytical results are summarized in Figs 4-7. The samples with the highest field temperatures and silica concentrations occurred in Crater Canyon ("SP001" at 30.2˚C and 470 mg/L silica, "626" at 22.3˚C and 230 mg/L silica, and "532" at 22˚C and 260 mg/L silica).

Water samples can be separated into three groups based on concentrations of chemical species: thermal waters, dilute waters and glacial melt, and dilute or mixed waters. These classifications seem to match field observations and stable isotope results.

Thermal waters had the highest measured field temperatures, highest overall concentrations chemical species, and highest alkalinity, TDS, and conductivity. These samples have $\delta^{18}O$ values that plot up to 1.5‰ heavier than the MWL, $\delta^{13}C$ values

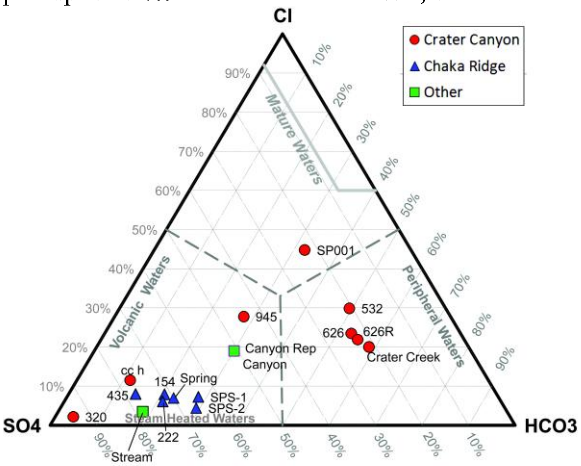

Figure 4. Anion ternary diagram showing composition of Spurr waters. Most samples have high sulfate or bicarbonate content, indicating that shallow processes are affecting the chemistry. A possible mixing trend can be seen between the highest temperature samples.

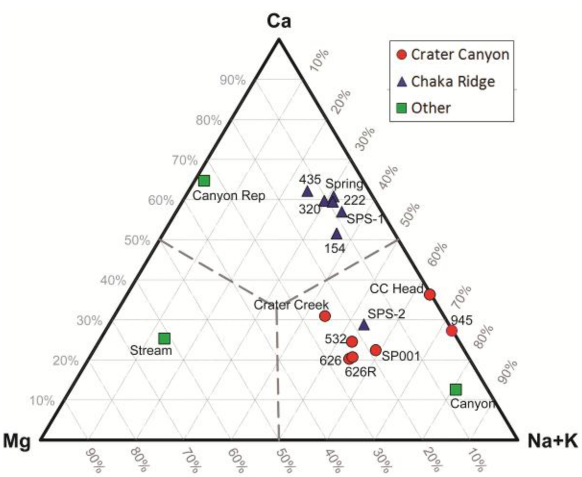

Figure 5. Cation ternary diagram showing composition of Spurr waters. Samples "Canyon" and "Canyon Rep" (a duplicate analysis of "Canyon") have very different Na value—the lower value of the Rep is more likely. Plot modified from spreadsheet by Powell, 2010.

that are near 0‰, and moderately positive $\delta^{34}S$ values. All of these samples are from Crater Canyon, and are interpreted to represent waters from Crater Peak that have mixed with or been diluted by other shallow waters before re-emerging downslope as springs or seeps. Thermophilic yellow Monkey Flowers grow in the talus at the bottom of Crater Canyon, specifically near where "SP001" and "532" were sampled, and along Crater Creek. Sample "626" was collected from a massive algae-covered edifice that was seeping water, and there were also algae in Crater Creek and on the "SP001" seep.

Dilute waters and glacial melt waters had low measured field temperatures, low concentrations of chemical species, plot near the meteoric water line (MWL), and have variable, slightly negative, $\delta^{13}C$. $\delta^{34}S$ values are mostly near 0‰. Most of these samples were collected from cold seeps on Chaka Ridge that issue from pumice slopes and talus; "CC Head" was collected from a spring issuing from talus midway up the north wall of Crater Canyon, and "945" represents water flowing out from beneath the melting Kidazgeni glacier.

Dilute or mixed waters lie somewhere in between the other groups. They have low-moderate field temperatures and concentrations of chemical species, $\delta^{18}O$ values that plot about 0.5‰ to the right of the MWL (Fig. 7), moderately negative $\delta^{13}C$ values and variable positive $\delta^{34}S$ values. These samples are not spatially related, but can be interpreted in the context of where they occur. Sample "320" was collected in Crater Canyon, midway up the western canyon slope, and represents more diluted/mixed waters than the other samples from nearby. It is believed that thermal endmember fluid originating from Crater Peak is following faults or fractures that do not coincide with this sampling location, or that this sampling location is diluted by glacial meltwater to a greater extent than other locations. The sample "Canyon" was collected from a spring issuing from talus on a canyon floor between Crater and Kid Canyons. The sample Stream was collected at a topographic change between alder forest and the Chakachatna River, and issued from a soil slope. Acid springs have been observed along the stream bank about 4km upstream from this location, but were not flowing at the time of sampling.

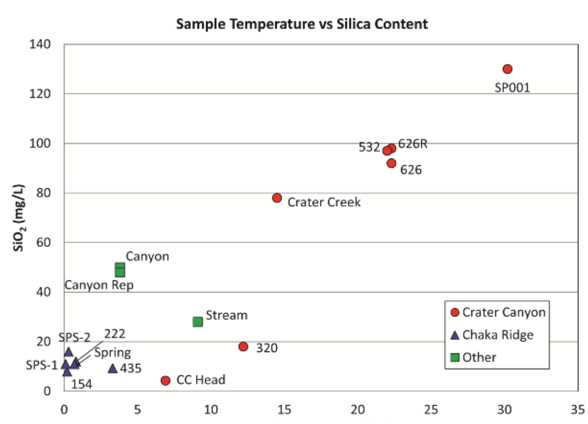

Figure 6. Sample temperature vs. silica content of Spurr waters. In general, silica content increases with temperature in a linear manner.

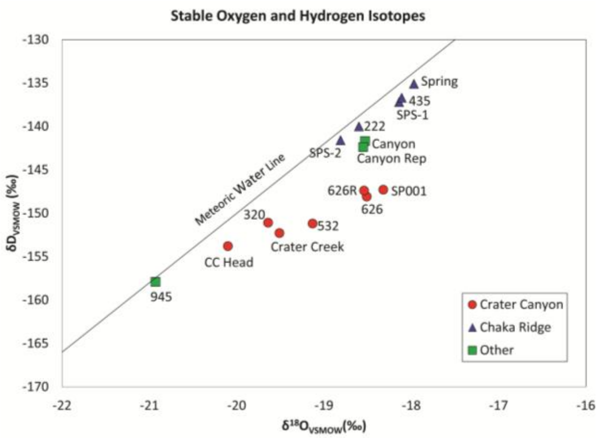

Figure 7. Stable oxygen and hydrogen isotopes of Spurr samples. Shifting of samples to the right of the meteoric water line indicates water-rock interaction and/or mixing with an andesitic water endmember.

<u>Thin Section Analysis</u>

The overall appearances of samples are consistent with previous general lithological descriptions (Calderwood and Frackler, 1972; Finzel et al, 2009; and Ormat Nevada, Inc., 2011). Clast types include light-colored granite, brown-gray andesite, a light colored fine grained rock that resembles quartzite or chert, pumice, a fine-grained dark colored rock that was probably originally volcanic but is now altered, some rocks that have relict glassy volcanic textures but are now altered, and foliated metamorphic rocks. Some clasts show rims of darker or lighter color around their circumference, indicating that some alteration reactions penetrated the outer parts of these clasts.

All thin sections showed evidence of post-depositional changes. Most clasts have undergone some alteration, but it is hard to constrain the timing of this because it may have occurred before the clasts were incorporated into the conglomerate. However, replacement of primary igneous minerals by biotite and chlorite is prevalent, and in some cases matrix grains, especially quartz, are broken, as shown in Figs 8-9. Calcite is very commonly seen in matrix as well as clast voids, and in veins that cross-cut both matrix and clasts. In clasts and matrix grains, epidote replaces the interior of plagioclase feldspar crystals. A Michel-Levy test on some albite-twinned feldspar in the matrix indicates the feldspar is predominately calcic in composition. No tartan twinning was observed. Additionally, a disseminated light and dark brown alteration can be seen in all thin sections. This alteration is associated with chlorite (bowlingite) and calcite, but also occurs in some clasts of presumed volcanic origin.

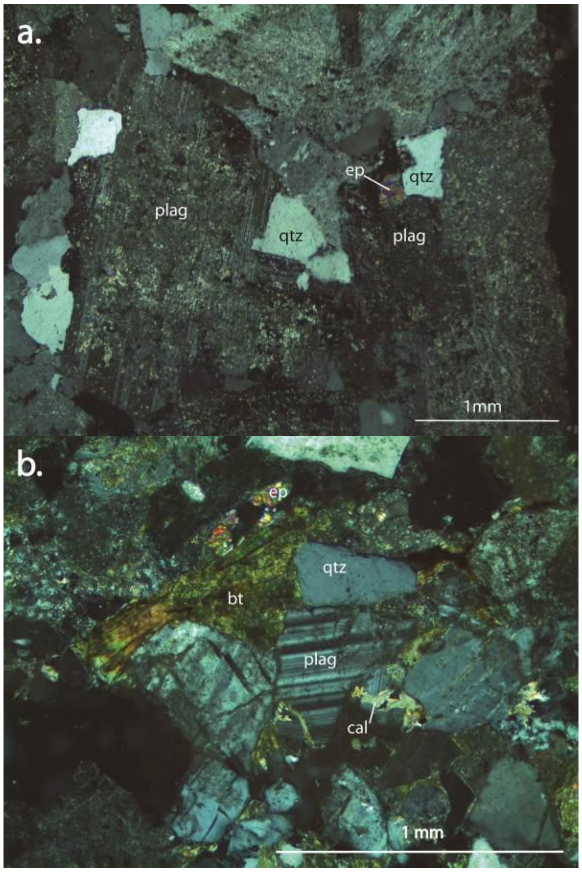

Figure 8. Photomicrographs of core from 26-11, crossed polars. a.) Epidote forming from altered feldspar in granitic clast at 682' depth. b.) Biotite and calcite in voids between matrix grains of feldspar and quartz. Also epidote replacing feldspar. From 3557' depth, sandy core.

<u>Clay Characterization</u>

Mineral constituents common to all the clay rich samples include quartz, plagioclase feldspar, and smectite. Three samples also contain some calcite. The clay has been identified as a dioctahedral montmorillonite-rich phase based on the 060 reflection. The sample "3434" also contained discreet chlorite. No illite or mixed-layer clays were identified.

The vein scraping predominately contains calcite, with some minor gypsum. No other carbonate phases were identified. The red material scraping is also predominately calcite, with minor quartz. However, no iron oxide minerals are represented in the diffraction patterns, though red material is plainly visible. This could be because the minerals are amorphous. Future work includes a treatment to increase the crystallinity of the amorphous oxyhydroxide by heating the sample to 900°C (Moore and Reynolds, 1997).

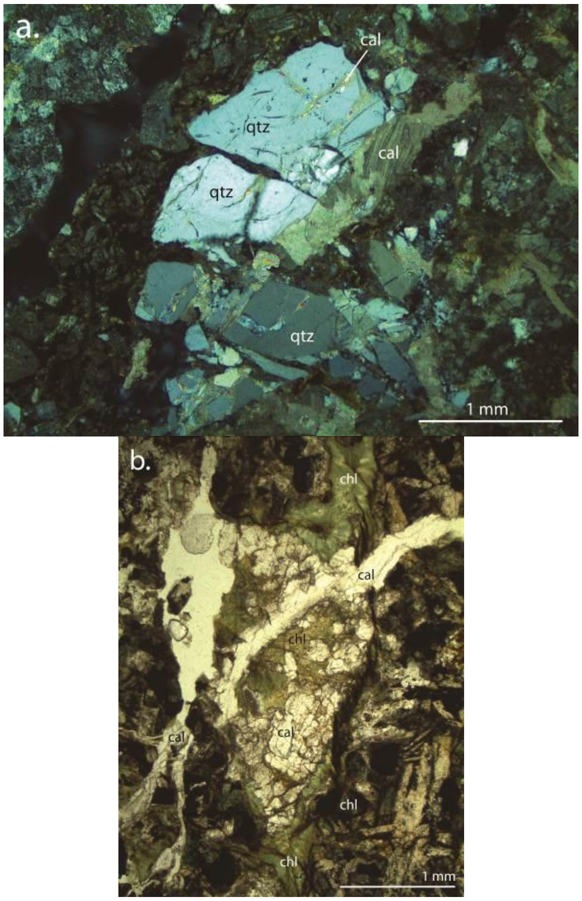

Figure 9. Photomicrographs of core from 26-11 at 3434' depth. a.) Fractured quartz grain with calcite in veins and voids in conglomerate matrix, crossed polars. b.) Void in volcanic clast infilled by calcite and epidote, plain light.

DISCUSSION

Aqueous Geochemistry

Major chemistry of thermal spring waters indicates that deep, magmatically influenced fluids are affected by shallow processes and likely mix with groundwater. This is shown by a positive linear correlation between Cl and B (Fig. 10) amongst thermal springs at Crater Canyon, as well as elevated SO_4 and HCO_3 concentrations (Fig. 4).

Acid-sulfate bicarbonate waters are produced when magmatic gasses (H_2S and CO_2) in steam encounter shallow water and are dissolved, which oxidizes the H_2S (Henley and Ellis, 1983).

Stable carbon and sulfur isotope results are shown in Fig. 11. The C and S isotopes of the samples from Chaka Ridge are compositionally variable, while samples from Crater Canyon are more similar to each other. All samples plotted near $\delta^{13}C=7$ (average

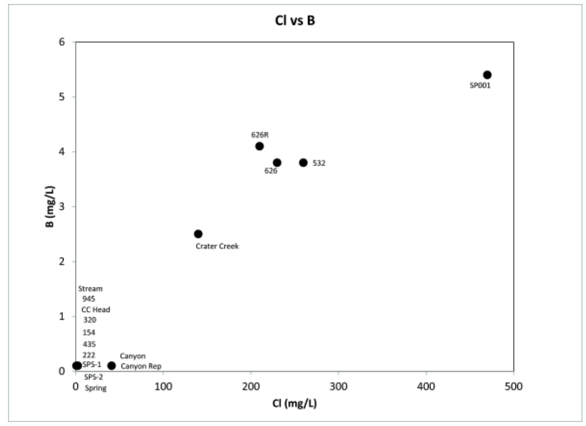

Figure 10. Chloride versus boron concentrations for all water samples collected in this research. A positive linear correlation is seen in the thermal waters from Crater Canyon.

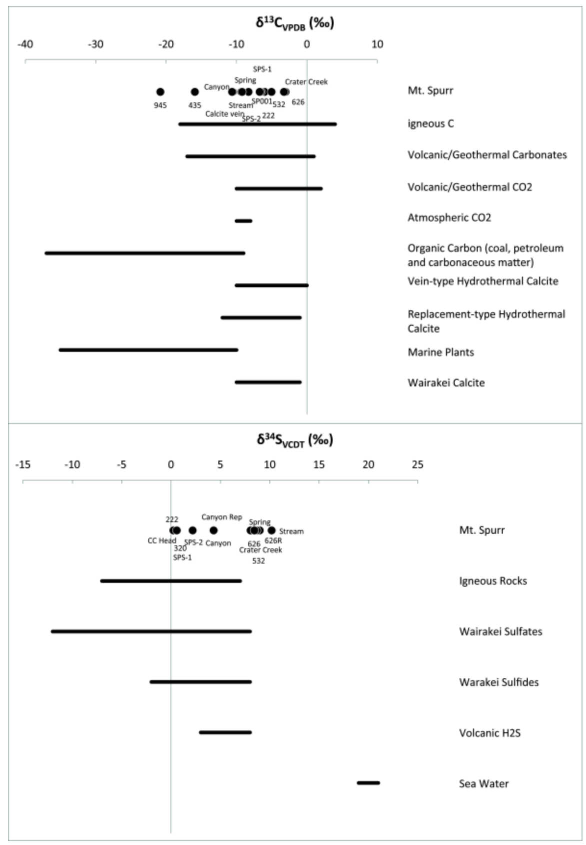

Figure 11. Stable carbon and sulfur isotopes from Mt. Spurr samples with data from Field and Fifarek, 1985 for comparison.

crustal carbon and atmospheric CO_2), except "435" and "945", which are more negative (Field and Fifarek, 1985). This clustering of most $\delta^{13}C$ values in the 0-5 permil range suggests a magmatic CO_2 origin.

The conceptual model proposed by Motyka and Nye (1993) for Mt. Spurr's hydrothermal system, shown in Fig. 12, is supported by the data of this research.

Samples from further afield, such as "Canyon" and "Stream" seem to have chemical compositions intermediate between the Crater Canyon samples and dilute or meteoric waters. Future efforts include basic geochemical modeling to see if the different water types can be related to one another along a reaction path.

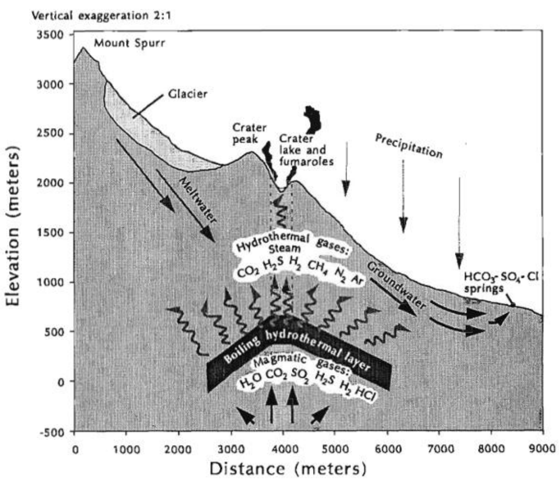

Figure 12. Conceptual model from Motyka and Nye, 1993. Magmatic gases rise from depth, encounter water, and either reach the surface as fumaroles or are further diluted and emerge as hot springs at more distal locations.

Petrology

The conglomerate and sandy units of core hole 26-11 have undergone brittle deformation, as seen by the fractured quartz and other grains, as well as at least one event of fluid infiltration, as shown by alteration of mafic minerals and calcite deposition. The brown alteration seen in the thin sections is believed to represent clay minerals that have been incorporated into the crystal structure of existing minerals. The sandy matrix likely allowed some initial permeability for fluids to enter and alter primary mafic minerals to biotite and chlorite. Four fault zones with clay mineral alteration and slikenlines, as well as calcite, chlorite, and iron oxide mineralization along fracture surfaces, were intersected during drilling of the core hole. It seems reasonable that the crushing of grains during faulting caused fracturing that allowed fluid to infiltrate the formation. As hydrothermal fluids rapidly rose to the surface, loss of steam and CO_2 by boiling could have caused the fluid to become supersaturated in calcite, triggering precipitation of calcite (Ellis, 1977).

The clay identified in all XRD scans is a montmorillonite-rich smectite phase, which could have been formed by weathering of volcanic glass (ash) or by hydrothermal alteration. Volcanic glass is easily altered and may decompose to opal, smectite, calcite, zeolite, or mixed layer clays (Henley and Ellis, 1983). Alteration to montmorillonite occurs at low temperatures, typically 100-175°C, whereas mixed-layer illite-montmorillonite occurs at higher temperatures 150-225°C (Henley and Ellis, 1983).

It has been demonstrated that di-octahedral smectite is the primary alteration product of andesitic lavas exuded by the submarine PACMANUS vent, and occurs at this location in interconnected perlitic cracks and vesicles (Giorgetti et al, 2006). The brown alteration seen in the thin sections of this research commonly occurs with calcite in a way that appears to represent replacement of primary vesicular texture. At Mt. Spurr, the presence of di-octahedral smectite could be similarly indicative of hydrothermal alteration. Beneath the smectite at PACMANUS, higher temperature phases including illite, chlorite, and mixed-layer clays were found at the upflow zones of hydrothermal fluids (Giorgetti et al, 2006).

Carbon and oxygen isotope data was also collected from a calcite occurring in a vein at 3434' depth ($\delta^{13}C_{PDB}$=-10.61, $\delta^{18}O$=-16.37). It has values comparable to those of the water samples, and in the range of observed volcanic/geothermal carbonates (Field and Fifarek, 1985). Future efforts include geochemical modeling of a calcite-saturated system to see how it may relate to the composition of spring waters.

Geothermometry

The application of solute-based liquid geothermometers to Mt. Spurr water samples is not reasonable because the waters are mixed and many of the assumptions inherent in the calculations are not met. The waters discharging at Mt. Spurr as springs and seeps probably do not represent a primary geothermal reservoir fluid because concentrations of chemical species indicate influence by shallow processes including deep steam absorption by shallow aquifers, mixing of these steam-heated waters with deep waters, and dilution of deep and mixed waters by meteoric waters. Additionally, montmorillonites of the West Foreland Formation could influence the concentrations of cations observed. Nevertheless, if we assume "SP001", the sample with the highest measured field temperature and silica concentration, is representative of a deeply sourced fluid and is minimally modified by fluid-rock interaction, the application of geothermometry yields temperatures of 127°C (chalcedony, Fournier and Potter, 1982), and 214°C (empirical Na-K-Ca, Fournier, 1981). High magnesium concentrations in SP001 result in nonsense negative values for Mg-corrected geothermometers underlining the extremely cooled and mixed nature of these fluids.

The aqueous and mineral geochemical results from this study indicate a shallow, heavily diluted hydrothermal system. Geophysical anomalies confirmed by drilling in 2010-2011 have shown mineralized fault zones on Chaka Ridge, as well as mineralized and clay altered fault zones and clay intervals to the south of Chaka Ridge. Clearly hydrothermal fluid flow has occurred at shallow depths in the past. The presence of clay minerals as the expression of a hydrothermally altered clay cap that overlies hot water instead of stratigraphically controlled weathered volcanic glass has huge exploration implications and requires additional investigation. Understanding faults as possible conduits or seals is important for the mapping of fluid pathways. The surface expression of a potential reservoir of hot water at Mt. Spurr is masked by intermediate bodies of water and meteoric/glacial meltwater dilution. Drilling deeper in a faulted area could reveal a deeper hydrothermal reservoir, but swelling clay is likely to be prevalent and problematic to penetrating the West Foreland Formation.

REFERENCES

Alaska Energy Authority, (2009). Renewable Energy Atlas of Alaska. http://www.akenergyauthority.org/Reports%20and%20Presentations/EnergyAtlas2009.pdf. Accessed 1/5/2012

Alaska State Long Term Energy Plans 1980-1982

Ellis, A.J. (1977). Chemical and isotopic techniques in geothermal investigations. *Geothermics* **5** 3-12

Field, C.W. and Fifarek, R.H. (1985) "Light stable isotope systematics in the epithermal environment," in Geology and Geochemistry of Epithermal Systems, vol. 2, Society of Economic Geologists.

Finzel, E. S., Gillis, R. J., Ridgway, K. A., and LePain, D. L. (2009). Preliminary evaluation of basin margin exhumation and provenance of Cenozoic strata, Chuitna and Beluga rivers area, Cook Inlet forearc basin, Alaska. Alaska Division of Geological and Geophysical Surveys Preliminary Interpretive Report 2009-4.

Fournier, R.O. (1981). "Application of water geochemistry to geothermal exploration and reservoir engineering," in Geothermal Systems: Principles and Case Histories. New York, NY: Wiley and Sons.

Fournier, R. O. and Potter (1982). A revised and expanded silica (quartz) geothermometer. *Geothermal Resources Council Bulletin* November 1982

Giorgetti, G., Monecke, T., Kleeberg, R., and Hannington, M.D. (2006). Low-temperature hydrothermal alteration of silicic glass at the PACMANUS hydrothermal vent field, Manus basin: an XRD, SEM and AEM-TEM study. *Clays and Clay Minerals*, **54** No. 2, 240-251

Henley, R.W., and Ellis, A.J. (1983) Geothermal systems ancient and modern: a geochemical review. *Earth-Science Reviews*, **19**, 1-50.

Martini, B.A., Lide, C., Owens, L., Walsh, P., Delwiche, B., Payne, A. (2011) Geothermal Resource Definition at Mt. Spurr, Alaska. *Geothermal Resources Council Transactions* **35**

Montgomery, S. L., and Barker, C. E. (2003). Coalbed methane, Cook Inlet, south-central Alaska: A potential giant gas resource. AAPG Bulletin, v. 87, **1**, 1-13.

Moore, D.M. and Reynolds, R.C. (1997) X-Ray Diffraction and the Identification and Analysis of Clay Minerals, 2nd Ed. New York, NY: Oxford University Press.

Motyka, R.J. and Nye, C.J. (1993) Fumarolic gas chemistry (1982) and thermal spring water chemistry, crater peak (1985), Mount Spurr, Alaska. *Short Notes on Alaskan Geology*. Alaska Department of Geological and Geophysical Survey Professional Report 113

Nye, C.J., and Turner, D.L. (1990). "Petrology, geochemistry and age of the Spurr Volcanic Complex, eastern Aleutian arc," *Bulletin of Volcanology*, **52**, 205–226.

Ormat Nevada, Inc., 2011; Drill records, logs, reports from Mt. Spurr Geothermal Exploration; Well 26-11 (or from 2010, Wells 62-2, 67-34); Tyonek Quadrangle, Alaska: Alaska Division of Geological & Geophysical Surveys Geologic Materials Center Data Report (pending)

Powell, T., Cumming, W. (2010). Spreadsheets for geothermal water and gas geochemistry. *Proceedings, Thirty-Fifth Workshop on Geothermal Reservoir Engineering, Stanford University* SGP-TR-188

Turner, D.L., and Wescott E.M. (1986). "Geothermal energy resource investigations at Mt. Spurr, Alaska," Geophysical Institute of the University of Alaska UAG R-308.

Waythomas, C.F., and Nye, C.J. (2002). "Preliminary volcano-hazard assessment for Mount Spurr volcano, Alaska," USGS OFR 01-482.